Cooperative chemotaxis of magnesium microswimmers for corrosion spotting

Ileana-Alexandra Pavel, Gerardo Salinas, Maciej Mierzwa, Serena Arnaboldi, Patrick Garrigue and Alexander Kuhn*

Dedication: This contribution is dedicated to the memory of Prof. Jean-Michel Saveant in recognition of his seminal contributions to the field of electrochemistry over many decades

Dr. I.-A. Pavel, Dr. G. Salinas, Dr. M. Mierzwa, Dr. S. Arnaboldi, P. Garrigue, Prof. A. Kuhn

Univ. Bordeaux, CNRS, Bordeaux INP, ISM, UMR 5255, F-33607 Pessac, France.

E-mail: kuhn@enscbp.fr

Supporting information for this article is given via a link at the end of the document.

Abstract: Numerous artificial micro- and nanomotors, as well as various swimmers have been inspired by living organisms that are able to move in a coordinated manner. Their cooperation has also gained a lot of attention because the resulting clusters are able to adapt to changes in their environment and to perform complex tasks. However, mimicking such a collective behavior remains a challenge. In the present work, magnesium microparticles are used as chemotactic swimmers with pronounced collective features, allowing the gradual formation of macroscopic agglomerates. The formed clusters act like a single swimmer able to follow pH gradients. This dynamic behavior can be used to spot in a straightforward way localized corrosion events. The autonomous docking of the swimmers to the corrosion site leads to the formation of a local protection layer, thus increasing corrosion resistance and triggering partial self-healing.

Introduction

In recent years, macro/micro and nanodevices able to transform fuel or external energy into motion have gained increasing attention.[1,2] From environmental issues[3] such as water treatment[4] and spilled-oil cleanup[5] to biomedical tasks,[6] from sensing and bio-sensing[7] to imaging,[8] and from simple structures to more complex ones,[9] these devices have numerous potential applications as they are very versatile. However, in practice, an individual particle, especially at the nanoscale, has only a limited capacity to accomplish a real task and reach the expected, often macroscopic goals. Therefore, the use of ensembles of such dynamic objects may be required in complex and changing environments.[10] The collective behavior of these artificial devices is often triggered by the input of external energy, such as light or magnetic forces, as well as by the presence of chemical stimuli. The latter case allows the swimmers to react to a chemical gradient and show chemotactic behavior.[11,12] Artificial chemotaxis in gradients of hydrogen peroxide, released from either a hydrogel,[13] a microfluidic device[14] or cells-macrophages,[15] have been reported. Gradients of surfactants,[16] of enzyme substrates[17] and pH[18] have also been used to generate more or less complex chemotactic behavior.[19-21] Concerning pH gradients, they can be triggered by several natural phenomena, such as enzymatic reactions[22-25] or, most importantly, corrosion events. We therefore explore in this contribution the idea whether the cooperative behavior of microswimmers can be used for detecting and spontaneous healing of local corrosion events.

We report the use of magnesium microparticles (Figure S1) as chemotactic swimmers that spontaneously self-organize and move in reaction to a local pH gradient generated by a corroding

piece of iron. The microswimmers not only present mutual attractive chemotactic behavior, leading to the formation of a cluster, but the resulting aggregate is also driving autonomously towards the site of corrosion and allows improving the corrosion resistance.

Corrosion of metals leads to the deterioration and eventually to complete destruction of a wide range of materials. In economic terms, the costs caused by corrosion represent about 3% of Gross National Product in industrialized countries.[26] A significant part of these costs concern corrosion detection and the design of materials with high corrosion resistance.

The detection of corrosion in early stages is essential in order to protect the metal from structural damage and function loss. There are various ways to fight against corrosion e.g. the use of specific coatings or galvanic protection. The latter is usually achieved by combining a metal having a rather negative electrochemical potential with the corroding metal. Zinc and magnesium are typically used as such sacrificial anodes. It is therefore interesting to explore the idea whether Mg microparticles might be used as active, dynamic compounds in this context.

Magnesium based swimmers have gained a lot of interest in the frame of numerous applications[27,28], such as drug[15,29,30] or hydrogen[31] delivery systems, removal of metal ions[32], degradation of organic pollutants[33] and cleaning of oil spills in sea water[34], because the only “fuel” that they require is water. They have shown propulsion towards pH and ionic strength gradients.[35] This positive chemotactic behavior is due to the tendency of magnesium to reach a thermodynamically more favorable state. Upon contact with water Mg starts to corrode leading to the oxidation of the surface and reduction of water to hydrogen bubbles.[36]

Anodic site: $Mg(s) \rightarrow Mg^{2+}(s)+2e^-$ (1)

Cathodic site $H_2O(l)+2e^- \rightarrow H_2(g)+2OH^-(aq)$ (2)

$Mg(s)+2H_2O(aq) \rightarrow Mg(OH)_2(s)+H_2(g)$ (3)

Results and Discussion

In the case of an isolated Mg particle, a magnesium hydroxide layer is forming at the metal surface, because $Mg(OH)_2$ has a low solubility product (ksp) of around 10^{-12} (mol l^{-1})3.[37] This layer slows down the overall reaction by passivating the surface of the individual Mg particle The presence of higher concentrations of acid [38], the use of catalytically active metals (like Au[34], Pt[39,40]) or even alloys[41], are strategies to increase hydrogen production and to power more efficiently the magnesium based motors. This leads to a higher speed, but also to shorter lifetimes, due to the fast consumption of the Mg core.[42] The high speed makes it also rather difficult to control precisely the direction of propulsion, which then mostly depends on the initial swimmer orientation.

In contrast, the behavior of the here presented isotropic swimmers is solely based on the natural oxidation kinetics of the magnesium as no other metal is present to catalyze it. As a result, the motion is quite slow and we have used this strategy on purpose, because in this case the microswimmers are much more sensitive to small pH gradients and consequently have also more time to reorient their trajectory. Thus, the slow reaction allows the swimmers to follow a local or global pH gradient, irrespective of their initial orientation.

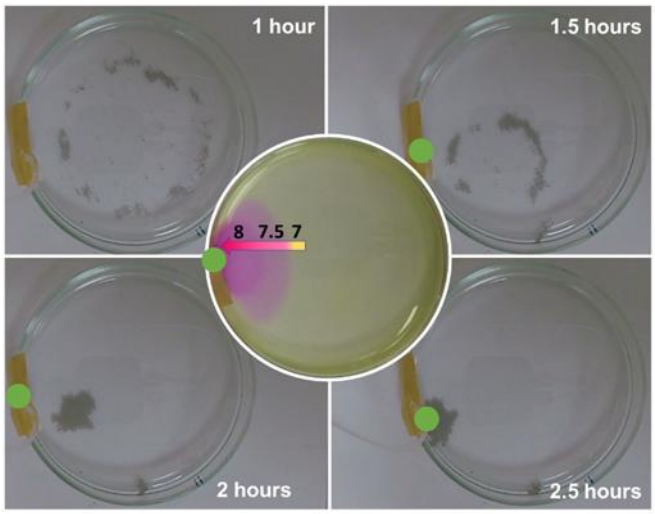

Figure 1. Time laps images of the behavior of the Mg microswimmers at the air/water interface in the presence of a base. The injection of the basic solution started one hour after the addition of Mg. Center: Illustration of the pH gradient (∇pH mm−1 ≈0.05) revealed by phenol red indicator 60 min after the beginning of the injection of a 0.1 mM KOH solution (0.05 ml/h). The green spot indicates the location of the microfluidic injection.

In the case of a particle ensemble, an OH- gradient is formed around each individual particle (Figure S2), which leads to mutual attraction. This is because Mg particles exhibit a positive chemotactic behavior with respect to OH- gradients as illustrated by Figure 1. Thus, the swimmers start to approach each other and form aggregates as shown in Video S1. This self-organization dynamics can be revealed when a certain amount of Mg microparticles is dispersed at the air/water interface of a Phenol red/SDS solution, acting as a pH indicator. In the first couple of minutes, the local change of pH towards more basic values occurs around each particle. Subsequently, the particles sense the ∇pH formed by the neighboring particles and approach each other, forming aggregates with a gradually increasing size, and finally merge into a single object. In the presence of a macroscopic basic gradient, generated by the addition of a 0.1 mM KOH solution at a rate of 0.05 mL h−1 (Figure 1 center), the newly formed cluster moves slowly towards the OH- source (Video S2).

Corroding metals in general produce pH gradients in their surroundings. Therefore, one can imagine using such pH sensitive microswimmers as active compounds migrating spontaneously towards a corroding surface. This would allow not only localizing a corrosion spot in a very visual way, but eventually also slowing down the corrosion kinetics via the formation of a local galvanic cell once they get in contact with the corroding object. We illustrate this concept with a model system based on a corroding piece of iron.

In contact with a solution containing oxygen, iron acts as an anode at certain spots and simultaneously as a cathode at other locations.

At the anodic section, the oxidation of iron takes place:

$$Fe(s) \rightarrow Fe^{2+}(aq) + 2e^- \quad (4)$$

At the cathode oxygen is reduced:

$$O_2(g) + 2H_2O(l) + 4e^- \rightarrow 4OH^-(aq) \quad (5)$$

producing the mentioned local pH gradient.

We therefore propose the experimental set-up illustrated in Scheme 1, using the microswimmers to spot the corroding iron via their directional movement towards the corrosion related OH- gradient.

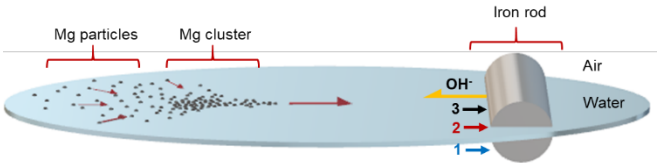

Scheme 1. Schematic representation of the magnesium cluster formation and the collective movement of the microswimmers towards the corroding iron. The corrosion is creating 3 distinct regions on the iron rod: R1-the area below the water level, R2-the triple junction air/water/iron and R3-the surface exposed to air.

In a first experiment, an approximately 1 cm long iron piece was positioned in the middle of a petri dish of 8 cm diameter, filled with 5 ml of SDS solution, thus covering the iron rod up to half-height, and left for 24 h. In parallel, another iron piece was placed in a second petri dish and approximately 2 mg of Mg microparticles were dispersed at the air/water interface. After 24h (Figure 2A1 and 2B1), both pieces were removed and left to dry in air for an hour. Scanning electron microscopy and EDS analysis were employed to characterize the magnitude of corrosion.

Three distinct regions can be observed on both samples (Figures 2A2-2A6 and 2B2-2B6). On the iron rod that was used as reference, region 1 (R1) that was totally immersed in water shows less signs of corrosion compared to region 2 (R2) at the air/water interface. This is due to the fact that the concentration of oxygen is higher at the interface, and therefore rust is formed more easily. Region 3 (R3) is the part that remained in air, and no corrosion is observed there.

In the case of the second iron rod that was corroding in the presence of the Mg microswimmers, these three regions are different. In R1 corrosion is almost insignificant, whereas at the air/water interface (R2), a crystalline structure is observed. As the microswimmer cluster approaches the iron rod, the local pH is progressively increasing alongside with the Mg^{2+} concentration, creating an ion supersaturation. This leads to precipitation,[43] and the formation of nanosheets, most likely composed of a mixture of MgO_2 and $Mg(OH)_2$.[44] The presence of $Mg(OH)_2$ is not only indicated by the crystal morphology and the EDS mapping of this part of the surface (Figure 2B6), but also by a significant decrease of corrosion rate in this area,[45] revealed by a less pronounced brown color on the right side of the rod (Figure 2B1).

In the next step, in order to test the capability of the microswimmer cluster to selectively spot localized corrosion, two iron rods of approximately 3 cm length were partially protected with white nail varnish, leaving a 1 cm long opening. After positioning them in 5 ml SDS solution, their behavior has been studied under two different conditions.

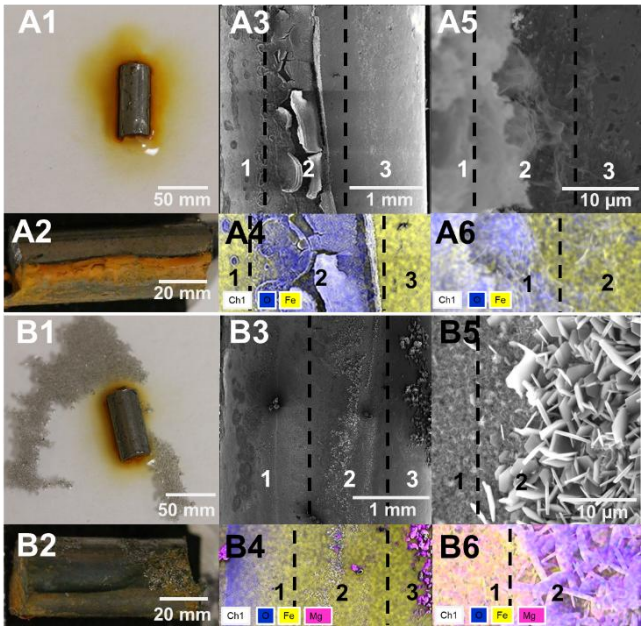

Figure 2. Corrosion of a 1 cm long iron rod after 24 h. Optical images showing typical corrosion of iron in a 0.125 mM SDS solution (A1/A2) in the absence and (B1/B2) in the presence of Mg microswimmers. Scanning electron micrographs and EDS maps of the two surfaces at different magnifications: A3/A4 and A5/A6 for the reference experiment, B3/B4 and B5/B6 for the Mg microswimmer protected rod. The numbers 1, 2 and 3 refer to the regions on the iron rod indicated in Scheme 1.

For a visual comparison of the localized corrosion of the rods during a 24h experiment, the KorroPad method was used. This method employs an agar-based gel, containing 0.1 M NaCl, as electrolyte and 1 mM K3[Fe(CN)6]. While NaCl initiates pitting corrosion at surface defects and imperfections, K3[Fe(CN)6] causes an anodic polarization of the surface (+275 mV Ag/AgCl on platinum). The released Fe3+ ions react with K3[Fe(CN)6] to form Prussian blue, allowing an easy localization and visualization of the corrosion by the intensity of the blue color.[46] After about one hour, a very small blue spot appears in the agar gel (Figure 3A1) that slowly grows over time only at the unprotected section of the rod (Figure 3A2).

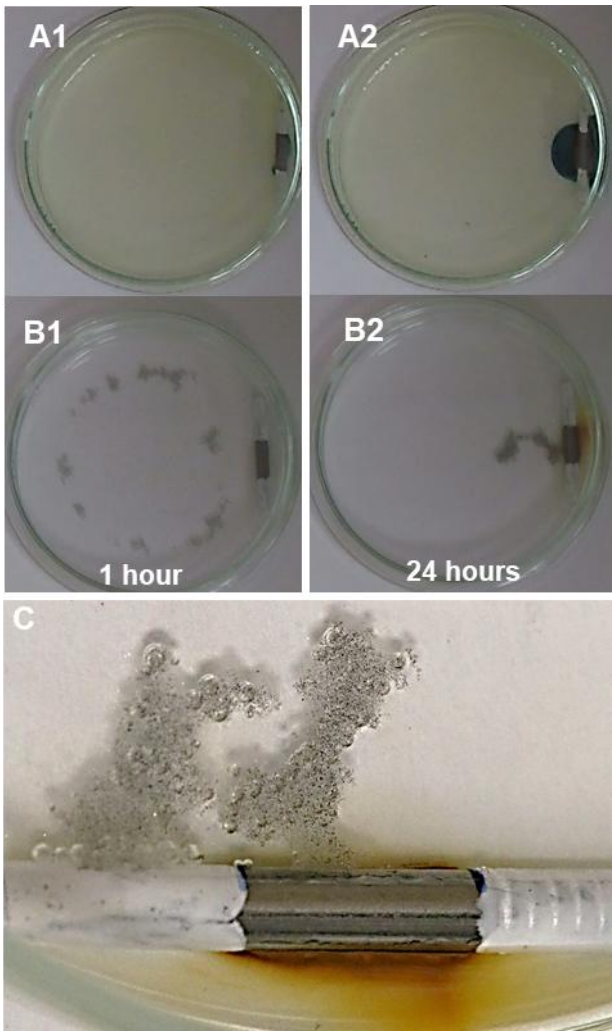

Figure 3. Corrosion experiment with two partially protected iron rods. A) KorroPad-testing of one iron rod after 1 (A1) and 24 h (A2) in 0.1 M NaCl/ 1 mM K3[Fe(CN)6] in agar gel. Corrosion of a second rod in a SDS solution in the presence of Mg microswimmers after 1 (B1) and 24 h (B2). C) Zoom of the rod from B2, illustrating the asymmetric progression of the corrosion by the distribution of the brown color.

A similarly easy visualization of the active corrosion site is possible by using the microswimmers without the need to employ a gel. Within minutes after exposing the iron rod to the solution and adding the Mg particles, the individual swimmers start to partially aggregate (Figure 3B1) and slowly move collectively towards the local OH- gradient generated by the active corrosion site. After approximately two hours, all the aggregates merge into a single one located in the vicinity of the unprotected section of the iron rod (Figure 3B2), thus providing a clear visual indication of the active corrosion site (Video 3). Afterwards metallic magnesium continues to dissolve and generates Mg(OH)2 in the local basic environment (vide supra). As in the previous experiment, this precipitate is not only localized on the Mg surface but also on the iron rod, leading to a spatially confined passivation. The resulting decrease of corrosion kinetics can be clearly seen from the asymmetric distribution of the brown color in Figure 3C. An examination of the surface by SEM/EDS (Figure 4) shows the corrosion patterns on the iron surface and the presence of magnesium after washing the samples. A pristine iron rod, that was just kept in air and used as an internal reference, has a homogeneous and slightly oxidized surface (Figure 4A1/A2). The second sample was half immersed in

the solution for 24h and the three regions depicted in Scheme 1 have been analyzed (Figure 4B1/B2). R1 has a rather rough aspect due to the significant formation of rust up to the limit of R2, corresponding to the air/water interface. Figure 4C1/C2 finally illustrates the corrosion state of the sample which was also exposed for 24h to the SDS solution, but in the presence of the microswimmers. As can be seen, this rod surface also has three distinct regions. Magnesium is present in R1, and in even bigger amounts at the triple junction air/water/iron (R2), whereas R3 shows as expected no significant signs of corrosion. However, even in this experiment, despite the presence of the microswimmers small signs of corrosion can be still observed which is probably due to the fact that the swimmer cluster needs almost 2 hours to reach the iron rod before protecting it against oxidation. By comparing regions 1 and 2 for the samples 2 and 3, one can conclude that the presence of the microswimmers significantly slows down the local corrosion kinetics, as it is also confirmed by the absence of brown color on the docking site of the swimmer cluster in Figure 3C.

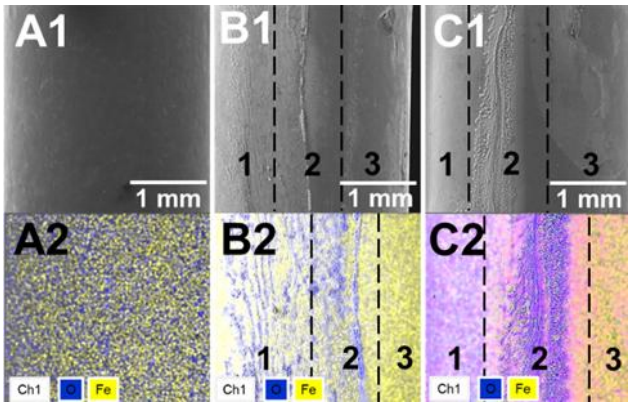

Figure 4. SEM/EDS analysis of: A1/A2, a pristine iron rod just stored in air; B1/B2, an iron rod kept in SDS solution for 24 hours; C1/C2, a rod exposed to SDS solution for 24h in the presence of the Mg microswimmers. The numbers 1, 2 and 3 refer to the regions on the iron rod indicated in Scheme 1.

Conclusion

In conclusion, we have demonstrated an easy and direct method for the visual recognition of iron corrosion by using self-powered magnesium microswimmers. The swimmers spontaneously agglomerate due to their positive mutual chemotaxis due to the basic pH gradient generated locally around every particle. After formation of a macroscopic single cluster, the latter is attracted by the active corrosion site of an iron rod and decreases the local corrosion kinetics by forming a magnesium hydroxide layer at its surface.

The chemotaxis of the microswimmers has been used in the present work for spotting active corrosion sites, but one can easily imagine that the concept can be extended to other (bio)chemical systems where local pH changes occur e.g. around biological cells. This would allow, among others a discrimination between living and dead cells. Therefore, this simple approach opens interesting perspectives for the further development of analog dynamic systems.

Experimental Section

All the experiments were performed in 8 cm diameter glass Petri dishes, containing 5 ml of a 0.125 mM sodium dodecylbenzenesulfonate (Sigma Aldrich) solution, unless stated otherwise.

To test the chemotactic behaviour of the magnesium swimmers, an artificial pH gradient was generated by the addition of a 0.1 mM KOH (Sigma Aldrich) solution at a constant rate of 0.05 ml/h

by a single-syringe pump (KDS100CE, kdScientific). The addition has been started one hour after approximately 2 mg of magnesium powder (with a rather large size distribution, ranging from 1 to 100 µm, 99,8 % purity, Laborden) were dispersed manually at the air/water interface. To illustrate the evolution of the pH gradient as a function of time, for both the artificial gradient and for the gradient formed by the Mg swimmers, 1.27 10-4 M Phenol Red ('Baker') was used as an indicator in the solution of SDS.

Commercially available iron rods, 3.1x70 mm (TREFIL), were cut in pieces with the desired length. They were carefully cleaned with acetone and paper wipes (Kimtech Science) before use. To prove the ability of the microswimmers to spot the corroding iron via their directional movement towards the corrosion related OH- gradient, 1 cm long iron rods were used. For the detection of localized corrosion, iron rods of approximately 3 cm length were partially protected with commercially available white nail varnish, leaving a 1 cm wide opening. The rods were placed in the glass petri dish, and covered up to half-height with SDS solution. After dispersing the Mg powder manually at the air/water interface, the Petri dish was covered with a glass cap in order to avoid water evaporation during the 24 h experiments.

The KorroPad method, used for the visualisation of the corrosion, consisted of an agar based gel-electrolyte containing 0.1 M NaCl (Acros), 1 mM K3[Fe(CN)6] (Sigma Aldrich) and 3 wt.% agar (Sigma Aldrich). All the ingredients were added in the appropriate amount to MilliQ water and brought to boiling under stirring. After the mixture had cooled down to 40-50 ºC, 5 ml of it were poured into the Petri dish and the iron rod was added. The experiments were recorded by a digital camera (GoPro Hero 5 Black) at 1 frame every 5 seconds. The videos where then processed with Image J software and converted to MP4 format. Scanning electron microscopy was performed on Tescan Vega3-SBH with an EDS detector (Bruker Detector XFlash 630M).

Acknowledgements

This project has been funded by the European Research Council (ERC) under the European Union's Horizon 2020 research and innovation program (grant agreement no 741251, ERC Advanced grant ELECTRA).

Keywords: microswimmers • collective behavior • corrosion •chemotaxis

[1] M. Fernández-Medina, M. A. Ramos-Docampo, O. Hovorka, V. Salgueiriño, B. Städler, Adv. Funct. Mater. 2020,30, 1908283.

[2] J. Katuri, X. Ma, M. M. Stanton, S. Sánchez, Acc. Chem. Res. 2017, 50, 2–11.

[3] J. Parmar, D. Vilela, K. Villa, J. Wang, S. Sánchez, J. Am. Chem. Soc. 2018, 140, 9317–9331.

[4] S. Shivalkar, P. K. Gautam, S. Chaudhary, S. K. Samanta, A. K. Sahoo, J. Environ. Manage. 2021, 281, 111750.

[5] T. D. Minh, M. C. Ncibi, V. Srivastava, B. Doshi, M. Sillanpää, Chemosphere 2021, 271, 129516.

[6] A.-I. Bunea, R. Taboryski, Micromachines 2020, 11, 1048.

[7] M. Pacheco, M. Á. López, B. Jurado-Sánchez, A. Escarpa, Anal. Bioanal. Chem. 2019, 411, 6561–6573.

[8] G. T. van Moolenbroek, T. Patiño, J. Llop, S. Sánchez, Adv. Intell. Syst. 2020, 2, 2000087.

[9] G. Salinas, I.-A. Pavel, N. Sojic, A. Kuhn, ChemElectroChem 2020, 7, 4853–4862

[10] H. Wang, M. Pumera, Chem. Soc. Rev. 2020, 49, 3211–3230.

[11] M. N. Popescu, W. E. Uspal, C. Bechinger, P. Fischer, Nano Lett. 2018, 18, 5345–5349.

[12] B. Liebchen, H. Löwen, Acc. Chem. Res. 2018, 51, 2982–2990.

[13] Y. Hong, N. M. K. Blackman, N. D. Kopp, A. Sen, D. Velegol, Phys. Rev. Lett. 2007, 99, 178103.

[14] L. Baraban, S. M. Harazim, S. Sanchez, O. G. Schmidt, Angew. Chemie - Int. Ed. 2013, 52, 5552–5556.

[15] J. Wang, B. J. Toebes, A. S. Plachokova, Q. Liu, D. Deng, J. A. Jansen, F. Yang, D. A. Wilson, Adv. Healthc. Mater. 2020, 9, 1901710.

[16] T. Toyota, N. Maru, M. M. Hanczyc, T. Ikegami, T. Sugawara, J. Am. Chem. Soc. 2009, 131, 5012–5013.

[17] J. Agudo-Canalejo, P. Illien, R. Golestanian, Nano Lett. 2018, 18, 2711–2717.

[18] K. K. Dey, S. Bhandari, D. Bandyopadhyay, S. Basu, A. Chattopadhyay, Small 2013, 9, 1916–1920.

[19] I.-A. Pavel, G. Salinas, A. Perro, A. Kuhn, Adv. Intell. Syst. 2020, 3, 2000217.

[20] J. Plutnar, M. Pumera, Angew. Chemie - Int. Ed. 2019, 58, 2190–2196.

[21] W. Wang, W. Duan, S. Ahmed, T. E. Mallouk, A. Sen, Nano Today 2013, 8, 531–554.

[22] R. Villalonga, P. Díez, A. Sánchez, E. Aznar, R. Martínez-Máñez, J. M. Pingarrõn, Chem. - A Eur. J. 2013, 19, 7889–7894.

[23] A. Llopis-Lorente, B. de Luis, A. García-Fernández, P. Díez, A. Sánchez, M. D. Marcos, R. Villalonga, R. Martínez-Máñez, F. Sancenón, J. Mater. Chem. B 2017, 5, 6734–6739.

[24] B. de Luis, Á. Morellá-Aucejo, A. Llopis-Lorente, T. M. Godoy-Reyes, R. Villalonga, E. Aznar, F. Sancenón, R. Martínez-Máñez, Chem. Sci. 2021, 12, 1551–1559.

[25] J. P. Byers, M. B. Shah, R. L. Fournier, S. Varanasi, Biotechnol. Bioeng. 1993, 42, 410–420.

[26] I. Gurrappa, I. V. S. Yashwanth, in Intell. Coatings Corros. Control (Eds.: A. Tiwari, J. Rawlins, L.H. Hihara), Elsevier Inc., 2015, pp. 17–58.

[27] C. Chen, E. Karshalev, J. Guan, J. Wang, Small 2018, 14, 1704252.

[28] B. Jurado-Sánchez, M. Pacheco, R. Maria-Hormigos, A. Escarpa, Appl. Mater. Today 2017, 9, 407–418.

[29] B. Esteban-Fernández de Ávila, P. Angsantikul, J. Li, M. Angel Lopez-Ramirez, D. E. Ramírez-Herrera, S. Thamphiwatana, C. Chen, J. Delezuk, R. Samakapiruk, V. Ramez, M. Obonyo, L. Zhang, J. Wang , Nat. Commun. 2017, 8, 272.

[30] F. Zhang, R. Mundaca-Uribe, H. Gong, B. Esteban-Fernández de Ávila, M. Beltrán-Gastélum, E. Karshalev, A. Nourhani, Y. Tong, B. Nguyen, M. Gallot, Y. Zhang, L. Zhang, J. Wang, Adv. Mater. 2019, 31, 1901828.

[31] K. Liu, J. Ou, S. Wang, J. Gao, L. Liu, Y. Ye, D. A. Wilson, Y. Hu, F. Peng, Y. Tu, Appl. Mater. Today 2020, 20, 100694.

[32] D. Zhang, D. Wang, J. Li, X. Xu, H. Zhang, R. Duan, B. Song, D. Zhang, B. Dong, J. Mater. Sci. 2019, 54, 7322–7332.

[33] B. Jurado-Sánchez, S. Sattayasamitsathit, W. Gao, L. Santos, Y. Fedorak, V. V. Singh, J. Orozco, M. Galarnyk, J. Wang, Small 2015, 11, 499–506.

[34] W. Gao, X. Feng, A. Pei, Y. Gu, J. Li, J. Wang, Nanoscale 2013, 5, 4696–4700.

[35] G. Salinas, A. L. Dauphin, C. Colin, E. Villani, S. Arbault, L. Bouffier, A. Kuhn, Angew. Chemie 2020, 59, 7508–7513.

[36] G. Song, A. Atrens, Adv. Eng. Mater. 2003, 5, 837–858.

[37] G. G. Perrault, J. Electroanal. Chem. Interfacial Electrochem. 1974, 51, 107–119.

[38] Y. Sun, M. Li, R. Duan, D. Zhang, H. Zhang, B. Song, B. Dong, Adv. Mater. Technol. 2018, 3, 1800208

[39] F. Mou, C. Chen, H. Ma, Y. Yin, Q. Wu, J. Guan, Angew. Chemie - Int. Ed. 2013, 52, 7208–7212.

[40] K. Xiong, L. Xu, J. Lin, F. Mou, J. Guan, Research 2020, 2020, 6213981.

[41] W. Gao, A. Pei, J. Wang, ACS Nano 2012, 6, 8432–8438.

[42] S. K. Srivastava, G. Clergeaud, T. L. Andresen, A. Boisen, Adv. Drug Deliv. Rev. 2019, 138, 41–55.

[43] A. Maltseva, V. Shkirskiy, G. Lefèvre, P. Volovitch, Corros. Sci. 2019, 153, 272–282.

[44] M. Liu, J. Xu, B. Cheng, W. Ho, J. Yu, Appl. Surf. Sci. 2015, 332, 121–129.

[45] Y. B. Hu, M. Zhang, R. Qiu, X. Y. Li, J. Mater. Chem. A 2018, 6, 2517–2526.

[46] N. Kauss, A. Heyn, T. Halle, P. Rosemann, Electrochim. Acta 2019, 317, 17–24.

Entry for the Table of Contents

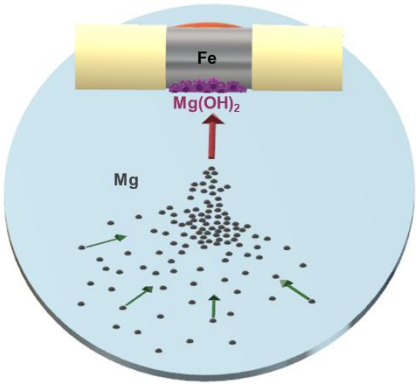

The collective behavior of magnesium microswimmers is used to identify corrosion by their self-assembly and docking to the active corrosion spot on an iron rod. The proximity between the resulting microswimmer cluster and the corroding metal further allows slowing down the local

corrosion kinetics. The concept can be generalized to other processes where local pH gradients are formed.